Evidence for Magnetic Reconnection in Three Homologous Solar Flares observed by RHESSI

Linhui Sui[1], Gordon D. Holman,

and

Brian R. Dennis

Laboratory for Astronomy and Solar Physics, Code 682, NASA Goddard Space Flight Center, Greenbelt, MD 20771

ABSTRACT

We present RHESSI observations of three homologous flares, which occurred between April 14 and 16, 2002. We find that the RHESSI images of all three flares at energies between 6 and 25 keV had some common features: (1) A separate coronal source up to $\sim 30''$ above the flare loop appeared in the early impulsive phase and stayed stationary for several minutes. (2) Before the flare loop moved upward, as previously reported by others, the flare looptop centroid moved downward for 2-4 minutes during the early impulsive phase of the flare, falling by 13-30% of its initial height with a speed between 8 and 23 km s^{-1}. We conclude that these features are associated with the formation and development of a current sheet between the looptop and the coronal source. In the April 14-15 flare, we find that the hard X-ray flux (> 25 keV) is correlated with the rate at which the flare loop moves upward, indicating that the faster the loop grows, the faster the reconnection rate, and therefore, the greater the flux of accelerated electrons.

Subject headings: Sun: flares—Sun: X-rays

1. Introduction

The motion of flare ribbons and loops is one of the clearest signatures of magnetic reconnection in the solar atmosphere. Decades of flare observations have shown the separation of

[1]Department of Physics, Catholic University of America, 620 Michigan Ave, Washington, DC 20064; lhsui@stars.gsfc.nasa.gov.

ribbons or footpoints and the apparent rise of hot plasma in magnetic loops. These motions have been interpreted as the continual propagation of the reconnection site to new, higher field lines (Kopp & Pneuman 1976).

It is widely accepted that magnetic reconnection occurs in the corona to power eruptive solar events. Because the features in the corona are hard to observe directly, many chromospheric observations have been conducted and analyzed in order to indirectly study this coronal magnetic reconnection. The often-observed flare ribbon separation in Hα and footpoint motion in hard X-rays (HXRs) are believed to be the chromospheric signatures of the progressive magnetic reconnection in the corona. The apparent motions reflect a shift of emission to neighboring footpoints of newly reconnected field lines (Krucker, Hurford & Lin 2003). The apparent velocity of the footpoints corresponds to the rate of magnetic reconnection in the current sheet. The model predicts that the speed of footpoint separation is directly related to the rate of magnetic reconnection in the corona. However, Sakao, Kosugi, & Masuda (1998) did not find a clear correlation between the speed of footpoint separation and the HXR flux in the 14 flares observed with the Yohkoh Hard X-ray Telescope (HXT). Several studies of the motion of footpoints in HXRs have been carried out with the Ramaty High Energy Solar Spectroscopic Imager (RHESSI, Lin et al. 2002). Fletcher & Hudson (2002) found systematic patterns of apparent footpoint motion, but the motions varied from flare to flare and did not resemble the simple increase of footpoint separation expected from 2D reconnection models. Krucker, Hurford & Lin (2003) studied the HXR source motions of the 2002 July 23 γ-ray flare. They found the motion of one foot point was correlated with the time profile of the HXR flux for that footpoint, but the motion of the other footpoint was too complicated to interpret in this way.

Decades of observations have also revealed the apparent upward motion of flare loops (Bruzek 1964; Švestka et al. 1987; Tsuneta et al. 1992; Švestka 1996; Gallagher et al. 2002). The observed lifetime of the growing loop system in X-rays is much longer than the radiative cooling time deduced from the loop density. Therefore, new, higher loops must be successively formed to keep the growing loop system visible in X-rays. The successive loop formation results from the upward motion of the magnetic reconnection site. The faster the reconnection rate, the faster the reconnection site moves upward.

Checking the correlation between the flare loop expansion rate and the HXR flux is an alternative test of the reconnection model. Testing this correlation has some advantages over studies of footpoint motions. When the flare images in X-rays do not show much footpoint emissions, such as the April 14-15 and 16 flares in this paper, the speed of footpoint separation is impossible to estimate. Moreover, the speed of footpoint separation is not only related to the magnetic reconnection rate, but also depends on the magnetic configuration in the

footpoint areas. If the magnetic flux is high so that magnetic field lines around the footpoints are very dense, then even at the peak of the flare, the separation speed could be very slow. If the magnetic flux is lower, as may be the case later in a flare, the continual reconnection would lead to a faster footpoint separation. By taking into account both the separation speed (V) and the normal component of the magnetic filed strength (B), Qiu et al. (2004) found a temporal correlation between the HXR flux and $V \times B$, which was believed to be related to the magnetic reconnection rate (Forbes & Priest 1984; Forbes & Lin 2000), in two flares.

Another interesting phenomenon is "loop shrinkage", first suggested by Švestka et al. (1987). Because of the short cooling time of hot, relatively dense plasma, the Hα loops were expected to be at heights very close to the heights of the X-ray loops. However, Švestka et al. found that the hot X-ray loops extend to much greater altitudes than the Hα loops. To explain this, they suggested that the hot X-ray flare loops shrink downward while cooling. The scenario they proposed starts with the magnetic field opening and subsequent field line reconnections. Immediately after reconnection, a cusp-shaped, non-potential loop is formed which subsequently shrinks to a potential configuration without a cusp. As the loops start to cool, the density increases due to chromospheric evaporation and the loops move to a lower altitude. Eventually the loop is observed in Hα at much lower altitudes. The shrinkage was revealed by comparing the height of nested flare loops seen at different wavelengths.

Forbes & Acton (1996) quantitatively studied the shrinkage of post-flare loops in two flares using the Yohkoh Soft X-ray Telescope (SXT). By using only soft X-ray observations, they did not need to consider the possibility that the observed shrinkage is just the result of the plasma cooling as did Švestka et al. (1987). The shrinkage they studied is mostly due to the change of the field line from a cusp to a rounded shape. Although the whole flare loop system expands with time, they found that the individual field lines shrank by about 20% and 32% for the two events they studied. Note that although the individual loops shrank, the whole loop system grew upward in the observations.

Recently Sui & Holman (2003) reported RHESSI observations of a 2002 April 15 flare. They found that the altitude of the looptop centroid decreased at ~ 9 km s^{-1} for about 3 mins in the early impulsive phase of the flare, and then increased at ~ 8 km s^{-1} later. The later altitude increase agrees with previous observations (Bruzek 1964; Švestka et al. 1987; Tsuneta et al. 1992; Švestka 1996; Gallagher et al. 2002). However, the altitude decrease of the looptop centroid has never been observed before, and it is different from the "loop shrinkage" studied by Švestka et al. (1987) or Forbes & Acton (1996) because their observations support the continual expansion of the whole loop system, i.e. the altitude of the looptop centroid should increase continuously.

In addition to the thermal flare loop, Sui & Holman (2003) found an extra coronal source which was initially connected with the loop at the looptop before the impulsive rise. The coronal source then separated from the loop at the start of the impulsive phase, and stayed stationary for about 2 minutes before moving outward. Based on the fact that the temperature of the underlying loops increased towards higher altitude, while the temperature of the coronal source increased towards lower altitude, Sui & Holman proposed that this was evidence for a large-scale ($\sim 1.2\times10^4$ km) current sheet between the top of the flare loops and the coronal source during the impulsive phase.

In this paper, we present RHESSI observations of three consecutive flares from the same active region, including the flare on 2002 April 15 discussed by Sui & Holman (2003). The detailed analysis of these three flares supports the previous findings.

2. Observations

The period from 14 to 21 April 2002 was a time of moderate to high solar activity, due mainly to the transit across the disk of three large active regions NOAA: 9901, 9906 and 9907 (Gallagher et al. 2002). We have analyzed the RHESSI observations of all three major flares (> M1) that occurred in active region 9901 from 14 to 16 April 2002 (Table. 1), as it approached the northwest limb. All three flares occurred within $\sim10''$ in latitude and $\sim30''$ in longitude of one another after allowing for solar rotations; they have similar light curves and morphological appearance, so can be considered homologous. The RHESSI thin attenuators (Smith et al. 2002) were in place throughout the observations of all three flares, thus limiting the lower energy of the X-ray observations to $\sim$ 6 keV.

2.1. M3.7 Flare on 2002 April 14-15

RHESSI X-ray light curves in two energy bands (6-12, 25-50 keV) are shown in Figure 1 (*top panel*). The flare had a typical gradual rise and fall in SXRs. The impulsive phase had multiple spikes, and lasted about 12 min. The HXR flux (> 25 keV) increased abruptly at 00:00 UT, then decayed slowly after the impulsive phase.

Four of the RHESSI CLEAN images (Hurford et al. 2002) at 12-25 keV around the start of the impulsive phase are shown in Figure 2. The RHESSI images in the 6-12 and 12-25 keV energy bands are interpreted as showing a flare loop with a bright looptop. In addition to the obvious flare loop, there is a faint coronal source above the loop in the first three images. The coronal source did not appear in the images before 00:00 UT on April

15 and its location did not change with time. This faint coronal source is distinct from the Masuda-type looptop HXR coronal source (Masuda et al. 1994) in the following aspects: (1) the Masuda source typically appears in the HXR images at energies above the Yohkoh HXT M1-band (22-32 keV) (Masuda et al. 1995); (2) the Masuda source is usually located a few arcseconds above the SXR looptop, while the faint coronal source in Figure 2 is located much higher above the loop, almost 30″ away from the centroid of the looptop.

The RHESSI 25-50 keV images during the impulsive phase most show a bright looptop, which may be due to thick-target bremsstrahlung from electron beams collisionally stopped within the loop due to very high loop column densities (Veronig & Brown 2004; Veronig et al. 2004). Some of the 25-50 keV images also show very faint footpoints. A sample 25-50 keV image at 00:01:20 UT is plotted in Figure 2.

Since the flare loops in the 6-12 and 12-25 keV images consistently have a bright looptop, we have used the centroid of the flux within the 60% contour to quantify the location of the looptop source. The altitude of the looptop centroid is defined, in the plane of the sky, as the distance between the centroid of the looptop and the center of the line between the two footpoints. The altitude of the looptop centroid in the following two flares was obtained in the same way. The correction for projection effects is neglected because all three events occurred close to the northwest limb, giving only a 10-20% error assuming the flare loop is perpendicular to the surface of the Sun. In this paper, we are only interested in the altitude variation of the centroids, so this error will not compromise our study. Figure 3 shows the altitude history of the looptop centroid. Due to the low count rate in the rise phase of the flare, the integration time of the images was 1 min before 00:00 UT and 20s after.

Although the resolution of the images in Figure 2 is 7″, the centroid can be determined with an accuracy of less than one arcsecond from RHESSI images. When the count rate was low in the rise phase of the flare, however, the loop morphology in the RHESSI images varied from frame to frame. This results in larger errors in determining the location of the looptop centroid. So far, we have not found a good way to estimate errors in determining the centroid location for RHESSI images, except for the Back-Projection images reconstructed with a single grid (Hurford et al. 2003). Image simulation using RHESSI simulation software might be a solution (Gordon Hurford, private communication). Therefore, in this paper, we limit our study of the behavior of the looptop centroids when the count rate was high enough ($\geq 10^4$ counts s^{-1}) so that RHESSI images with 20s integration time showed stable and consistent loop structure.

There are several notable features in Figure 3: (1) The altitude of the looptop centroid obtained from the 12-25 keV images is consistently higher than that from the 6-12 keV images. This indicates that hotter loops are located higher than cooler loops, in agreement with

previous Yohkoh SXT and RHESSI observations (Tsuneta et al. 1992; Tsuneta 1996; Gallagher et al. 2002; Sui & Holman 2003). This temperature distribution has been interpreted as evidence for energy release from magnetic reconnection above the top of the loop.

(2) Around the HXR impulsive rise of the flare (from 00:00 UT to 00:04 UT), the altitude of the looptop centroid decreased by 13% of the initial looptop altitude in the 6-12 keV images, and 20% in the 12-25 keV images. A linear fit gives downward speeds of 10 and 11 km s^{-1} for the 6-12 and 12-25 keV bands, respectively.

(3) After 00:04 UT, the looptop altitude increased continuously in both energy bands. The dashed line in the *lower panel* of Figure 3, which shows the speed of the looptop centroid in the 12-25 keV band, shows a correlation with the HXR flux at 25-50 keV. The average speed is about 20 km s^{-1} in period 'A', which is faster than the speed of $\sim$10 km s^{-1} in period 'B', when the HXR flux is lower. A sudden increase of the speed in period 'C' to $\sim$40 km s^{-1} correlates with the sudden increase of the 25-50 keV flux in this period although with a delay of 20-40s. The speed quickly decreases down to 5 km s^{-1} in period 'D' when the HXR flux was decreasing.

The downward and upward motions of the looptop centroids are also illustrated in Figure 4, where the locations of the looptop centroids, grey-coded by time, are plotted on the central region of the 00:01 UT 12-25 keV image shown in Figure 2. We notice that the looptop centroids in both the downward and the upward motions are clustered on a line, whose direction is far (about 53-56°) from the radial direction. The centroid initially moved away from the coronal source above the loop, and then moved toward the coronal source above the loop after 00:04 UT. The downward and the upward source motion is similar to that observed for the following two flares.

2.2. M1.2 Flare on 2002 April 15

The second flare occurred at the end of April 15, almost 24 hours after the first flare. RHESSI X-ray light curves in two energy bands (6-12, 25-50 keV) are shown in Figure 1 (*middle panel*). They are strikingly similar to those for the first flare in almost all aspects, except that the impulsive phase was shorter by a factor of $\sim$2.7 (only about 4 vs. 12 min).

RHESSI images at 10-25 keV are shown in Figure 5. Like the first flare, all the images at energies between 6 and 25 keV show a flare loop with a bright looptop. In the impulsive phase, the 25-50 keV images not only show a bright looptop source but also show two footpoints. A more comprehensive analysis of the event with multi-wavelength data is in preparation (Sui et al. 2004). Besides the flare loop, the first two images, which are before the

impulsive phase started, show a cusp-shaped coronal source with a rounded tip connected with the loop below. The shape of the coronal source is different from that of the cusps sometimes seen with Yohkoh SXT (Tsuneta et al. 1992; Tsuneta 1996), which usually have a more pointed tip. When the impulsive phase started, the coronal source separated from the underlying flare loop (Sui & Holman 2003). The coronal source then stayed stationary for about 2 minutes before moving outward at a speed of about 300 km s^{-1} soon after the major HXR peak of the flare at 23:11:40 UT.

Figure 6 shows the history of the looptop altitude obtained from the 6-12 and 12-25 keV images. The altitudes of the coronal source, obtained in the same way as the looptop altitude, are also plotted in Figure 6. In this figure, we find: (1) The loops in the 12-25 keV images are located consistently higher than at 6-12 keV, in agreement with Figure 3. (2) The looptop altitude in both energy bands decreases from the time of the HXR impulsive rise until the peak in SXRs around 23:12 UT. The altitude decreased about 24% of the initial looptop altitude in the 6-12 keV images, and 23% in the 12-25 keV loops. The indicated linear fits give speeds of 15 and 23 km s^{-1} for the 6-12 and the 12-25 keV bands, respectively. (3) Around the 6-12 keV peak of the flare at 23:12 UT, the looptop centroid started to move upward at speeds of 15 and 20 km s^{-1} for 6-12 and 12-25 keV, respectively. The downward and upward speeds obtained here are about two times faster than those obtained by Sui & Holman (2003). In that paper, the looptop centroids were obtained within a fixed rectangle surrounding the looptop region, while in this paper, the flux within the 60% contour of the looptop region was used to determine the centroid. The new method provides a more accurate tracking of the looptop motion. (4) The coronal source stayed stationary at altitude of $\sim$25 Mm when the looptop altitude was decreasing. It then moved outward at $\sim$300 km s^{-1} starting at 23:12 UT, the same time as the start of outward motion of the looptop centroid.

The downward and upward motions of the looptop centroids are also illustrated in Figure 7. Although the centroids showing the downward motion are more scattered, the looptop centroids in both downward and upward motions are still clustered on a line. The direction of the upward motion (13° from the radial direction) is closer to the radial than the downward motion (30° from the radial direction). Notice that the coronal source also changed its location to a more radial direction (see Fig. 5) when it started to move outward after 23:12 UT. This indicates that the looptop centroid moved either away from or toward the coronal source above the loop, which is consistent with the observations of the April 14 flare.

Among the three flares, this flare is the only one associated with a CME. Starting at 02:26 UT on April 16, SOHO/LASCO C2 and C3 observed a large coronal loop propagating at a constant speed of $\sim$ 300 km s^{-1}, i.e. the same as the speed of the RHESSI coronal

source after 23:12:09 UT. The large coronal loop in LASCO C3 images was too faint to be seen beyond 16 $R_\odot$. Assuming the coronal source in the RHESSI images continuously moved outward at 300 km s^{-1}, we estimated the location of the coronal source at 02:26:00 UT on April 16, when the large coronal loop was first seen in the LASCO C2 image. At that time the coronal source would have reached the inner edge of the coronal loop in the C2 image. Therefore, it is most likely that the outward moving coronal source is part of an ejected plasmoid (or a large-scale, helically twisted loop) with two ends anchored on the Sun, such as has been reported by Shibata et al. (1995) and Ohyama & Shibata (1998) using Yohkoh SXT.

2.3. M2.5 Flare on 2002 April 16

The RHESSI X-ray light curves of this flare in two energy bands (6-12, 25-50 keV) are shown in Figure 1 (*bottom panel*). They are very similar to those in the earlier two flares. There was a pre-impulsive burst at 13:03 UT. The impulsive phase lasted about 14 min.

Figure 8 shows a time sequence of 12-25 keV images immediately after the HXR impulsive rise (*top two rows*), and three 12-25 keV images at later times (*bottom row*). Since the count rate was low early in the impulsive phase, the integration time of images before 13:07:20 UT was extended to 1 min. Like the two earlier events studied above, RHESSI images below 25 keV show a flare loop with a bright looptop. The images between 13:03:20 UT and 13:06:20 UT also show a coronal source above the flare loop. Like the April 14 flare, most of the 25-50 keV images show only strong flare looptops. Two of them at the time of the major HXR peak at 13:11:30 UT show a weak northern footpoint. A sample 25-50 keV image at 13:10:20 UT is shown in Figure 8.

Compared with the two earlier flares, the coronal source in this flare is very bright relative to the looptop when the peak flux (indicated in Fig. 8) of the RHESSI 12-25 keV images is low. At 13:05:20 UT, in particular, the coronal source is almost as bright as the looptop. In the next image at 13:06:20 UT, although the flux of the coronal source above the loop did not change, the flux of the looptop increased by a factor of 3. This means that the coronal source was only $\sim 20\%$ as bright as the looptop. Therefore, later in the flare, the ratio of coronal to looptop source intensity became even smaller. The limited dynamic range of the RHESSI images ($\sim$10:1 with the present calibration) most likely explains why the coronal source disappeared from the images later in the flare.

Figure 9 shows the altitude-time profile of the looptop centroid and the coronal source above the looptop. Before the HXR impulsive rise at 13:06 UT, the altitude of the looptop

centroid increased steadily in both the 6-12 and 12-25 keV bands. This big altitude increase can also be seen clearly in Figure 8. The earlier RHESSI images show that loop emission came mainly from much lower altitudes than the loops in the later images. When the impulsive phase started, the looptop centroid in the two energy bands stayed at the same altitude for about 2 to 3 min before moving downward. That the loops maintain their altitudes around the impulsive rise was also suggested in the earlier two flares (see Fig. 3 and Fig. 6). We also notice that the altitude decrease in the two energy bands did not start simultaneously. The looptop altitude in the 12-25 keV band started to decrease about 1 min earlier than in the 6-12 keV band. This non-simultaneity in two energy bands is also indicated in the April 14-15 flare (see Fig. 3).

The looptop altitude in both energy bands decreased until 13:11:40 UT. The altitude of the looptop decreased about 16% of the initial altitude for the 6-12 keV loops, and 30% for the 12-25 keV loops. Linear fits give speeds of 8 and 12 km s^{-1} for 6-12 and 12-25 keV, respectively. Immediately after the major HXR peak at 13:11:40 UT, the looptop altitude in both energy bands started to increase with average velocities of 3 and 4 km s^{-1} for 6-12 and 12-25 keV, respectively. This is much slower than for the earlier two flares. Because of the relatively low velocities and the scatter in both energy bands, the correlation between the loop expansion rate and the HXR flux cannot be determined. Figure 10 shows the location of the looptop centroids for the 12-25 keV band plotted on the central region of the 12-25 keV image at 13:11:00 UT. Like the two earlier flares, the looptop centroids in both the downward and the upward motions are clustered along a line between 24° and 30° from the radial direction, and they moved first away from and then towards the coronal source above the looptop.

3. Discussions and Conclusions

We have presented RHESSI observations of three homologous flares from the same active region. Results are summarized in Tables. 1 and 2. The three flares share the following common features: (1) The looptop centroids altitudes of higher energy loops were at higher altitude than those of lower energy loops, indicating the hotter loops were above the cooler loops. (2) Around the start of the HXR impulsive phase, the altitude of the looptop centroid decreased with time, with the altitude in the 12-25 keV band decreasing more (except for the April 15 flare) and faster than that in the 6-12 keV band, (3) then the altitude increased with time later with velocities up to 40 km s^{-1}. (4) A separate coronal source appeared above the flare loop around the start time of the impulsive phase, and it stayed stationary for a few minutes. (5) The looptop centroid always moved along a direction which is either

away from or toward the coronal source above the loop.

Some of these features have been seen before. The altitude increase of flare loops has been reported by Bruzek (1964), Švestka et al. (1987), Tsuneta et al. (1992), and Švestka (1996). The temperature distribution of loops was seen by Moore et al. (1980), Švestka et al. (1987), and Tsuneta et al. (1992). The altitude increase of the looptops leads to the interpretation that the energy release occurred at higher and higher altitude in the corona. The observations of higher temperature loops located higher in altitude than cooler loops support the scenario of energy release above the top of the flare loops. At any given time, the outer, higher loops just formed are filled with hot plasma, whereas the inner, lower, loops were formed earlier, and have now cooled by radiation and conduction (Tsuneta 1996).

In the flare of April 14-15, we found a correlation between the loop growth rate and the HXR (25-50 keV) flux of the flare (Fig. 3), as expected in the classical reconnection model (Carmichael 1964; Sturrock 1966; Hirayama 1974; Kopp & Pneuman 1976). The faster the reconnection site moves up, the faster the reconnection rate. More energetic electrons are produced and, therefore, more HXR emission is observed. We found that the increase in the upward speed of the looptop source was delayed by 20-40 s with respect to the rise in the HXR flux. This time delay could be the time scale of the chromospheric evaporation. Observations have indicated that the speed of chromospheric evaporation at the impulsive phase of the major eruption varies from 300 to 800 km s^{-1} (Antonucci, Dodero, & Martin 1990, and references therein). For the April 14-15 flare, the loop height is about 30 arc sec (or 2.0×10^4 km), so it would take 20-60 s to fill a loop, in agreement with the RHESSI observation. Therefore, the flare loops may be formed by plasma evaporation due to an electron beam striking the lower atmosphere (for the flares with lots of footpoint emission in HXRs, such as the April 15 flare). Alternatively, they may be due to thermal conduction (for the flares with much less footpoint emission, such as the April 14-15 flare and the April 16 flare).

The previous observations indicated a continuous expansion of the flare loops (Bruzek 1964; Švestka et al. 1987; Tsuneta et al. 1992; Švestka 1996). The observations we present here show a different scenario. Early in the impulsive phases of the three flares, the looptop centroids move downward instead of upward. One possible explanation for this apparent downward motion is that the reconnection site moves horizontally along loops in an arcade toward Sun-center, giving the impression of an altitude decrease. However, the following points argue against this possibility: (1) By checking the time history of the footpoint centroids in the April 15 flare, which is the only flare with consistently strong footpoint emission in the impulsive phase, we did not find any systematic footpoint motion. (2) For all three events, the altitude decrease and the speeds of downward motion are often

significantly different in the 6-12 and 12-25 keV bands (see Table 2). This is in conflict with the assumption of motion along an arcade. (3) The non-simultaneous start of the downward motion of the looptop source in the 6-12 and 12-25 keV bands for both the April 14-15 flare and the April 16 flare also is in disagreement with this kind of motion along an arcade.

Our preferred explanation (Sui & Holman 2003) for the change in the measured position of the centroid is that the sources did, in fact, decrease in altitude early in the impulsive phase of all three flares. Based on the observational results, we propose two possible scenarios to explain this initial apparent fall of the looptop sources. Of course, some combination of these two scenarios could also be operating. Both scenarios assume that the energy is released above the loops by magnetic reconnection in the standard flare model, but use different mechanisms to explain the apparent downward motion. In the first scenario, the downward motion results from the relaxation of the newly reconnected field lines from a sharp cusp to a more semi-circular shape. This is similar to the model proposed by Švestka et al. (1987) and Forbes & Acton (1996) but on a much shorter time scale. The ∼2-4 min duration of the decrease in altitude in all three flares is consistent with the time taken for the loops to change their shape in this way (Lin et al. 1995; Lin 2004). In the second scenario, the initial downward motion results as the reconnection changes from slow X-point to the much faster Petschek-type (Petschek 1964). As this change takes place, not only would the energy release rate increase dramatically, consistent with the start of the impulsive phase, but also the lower bound of the current sheet would be pushed downwards, consistent with the observed initial decrease in altitude of the looptop source. In both scenarios, once the looptop source has reached a stable lower altitude where it can go no lower, the general rise of the current sheet would dominate over the other effects, and the centroid of the source would rise monotonically as higher and higher loops are created, in agreement with the observations for all three flares. In two of the flares (the flares on 15 and 16 April), this upward motion starts as the 25-50 keV flux begins to decay, suggesting a further transition in the reconnection process to the slower Sweet-Parker type (Parker 1957; Sweet 1958).

The downward motion of the looptop centroid early in the impulsive phase of the flares has only recently been recognized. The coronal source in the 2002 July 23 γ-ray flare also shows a noticeable downward motion early in the flare (see the right panel of Figure 3, Krucker, Hurford & Lin 2003). The recent event analyzed by Liu et al. (2004) using RHESSI data shows a similar of downward motion, suggesting that the downward motion of the looptop may be a common feature. Ultimately, the best way to show that the observed downward motion of the looptop centroid is a change in altitude is to search for similar effects in other flares at different locations on the solar disk, but that is beyond the scope of this paper.

The stationary coronal source above the flare loops has never been observed. A moving coronal source or plasma blob above flare loops has been observed before (see review by McKenzie 2002). The velocity of the coronal sources is in the range of 30-400 km s^{-1} (Shibata et al. 1995). One event on 1992 October 5 reported by Ohyama & Shibata (1998) had a plasma blob above a flare loop. The long-exposure SXT images revealed that the plasma blob was penetrated by or connected to the top of a large-scale loop. It was interpreted as a plasmoid (a large-scale helically twisted loop) resulting from magnetic reconnection. In the classical reconnection model (see review by McKenzie 2002), magnetic fields of opposing directions cancel out in the current sheet, and the tension that exists in the resulting non-potential field causes the expulsion of two oppositely directed jets. One jet appears as a plasmoid with embedded magnetic field moving upward, while the other downward directed jet piles up to form the arcade. Therefore, the outward moving coronal source or plasmoid is included in the model. Here we present a somewhat more complicated scenario. In the three events, a coronal source appeared near the time of the HXR impulsive rise, and was observed to stay stationary for 1∼2 mins before disappearing from the images (April 14-15 and 16 flares) or moving outward (April 15 flare). Since the three flares occurred in the same active region and seem homologous, it is reasonable to assume that the coronal source in the April 14-15 and April 16 flares would also have eventually moved outward. As discussed above, the reason we do not see them moving outward is probably due to the limited dynamic range of the RHESSI images.

Since the stationary coronal sources are usually much weaker than the flare looptop, we must consider the possibility that these coronal sources are artifacts of the imaging reconstruction process. The systematic variation of theses sources with time and energy argues against this. Simulations using RHESSI simulation software are in progress to determine at what level the artifacts might become important. These will be presented in a future paper.

There are many models of solar eruptive events: the kink instability and filament eruption model (Cheng 1977; Hood & Priest 1979), the tether cutting model (Moore & Roumeliotis 1992), the flux rope model (Priest & Forbes 1990; Forbes & Priest 1995; Lin & Forbes 2000; Lin 2002), the magnetic breakout model (Antiochos 1998; Antiochos, Devore, & Klimchuk 1999), the quadruple magnetic source model (Uchida et al. 1999; Hirose et al. 2001), etc. For the purpose of interpreting our observations, we use the flux rope model because it not only predicts magnetic reconnection in a current sheet above the observed hot flare loops, but it also predicts the evolution of the extended, long-lived current sheet. In their model, Forbes & Priest (1995) proposed that the converging photospheric flow or flux emergence leads to the formation of a sheared arcade field containing a flux rope. Two photospheric field sources approach each other until a catastrophe point is reached and the flux rope erupts. The eruption drives reconnection in a current sheet below the flux rope. If the rate

of reconnection is fast enough, the upward velocity can become high enough to allow the flux rope to escape and become a CME. The elongated current sheet can last for several hours and extend many solar radii into the outer corona (Ciaravella et al. 2002; Ko et al. 2003; Webb et al. 2003).

Some of the predications from the flux rope model agree with the observations. Sui & Holman (2003) interpreted the coronal source above the flare loop as the upper tip of a large-scale current sheet in the flux rope model. This was based on the temperature distribution of the coronal source in the April 15 flare, i.e. the higher temperature part located lower in altitude than the low temperature part. The model predicts that the speed of the upper tip of the current sheet is in the range of 200-700 km s^{-1} (J. Lin, private communication), in agreement with the observed speed (300 km s^{-1}) of the outward moving coronal source. We also observed the predicated upward motion of the looptop centroid later in the flares, suggesting the flare loops were formed continuously at higher altitudes. Although the angle between the direction of the upward motion and the radial direction varies (see the right panels of Fig. 4, Fig. 7, and Fig. 10), the loop always expanded toward the coronal source, agreeing with the flux rope model.

There are some observations which cannot be explained by the flux rope model or any of the other models in the literature. In the April 15 flare, when the HXR impulsive phase started, the coronal source separated from the underlying loop (Fig. 5). It is reasonable to assume that the system had lost its equilibrium at this point. The model predicts that the flux rope is continuously thrust upward after that time. However, the coronal source was observed to stay stationary for about 2 minutes before moving outward. So, what kept the plasma from moving outward early in the flare?

Since the downward motion of the looptop centroid occurs over the same time range that the coronal source remains stationary, we believe they are related to each other, and may be associated with the formation or development of the current sheet. So far, most of the models and simulations focus on the magnetic reconnection after it starts, and do not address how the current sheet is dynamically formed and evolves with time. Hopefully, the observations of the three flares presented here will be an incentive for more theoretical work in this regard.

We thank Edward Schmahl, Hugh Hudson, Jun Lin, and Gordon Hurford for their helpful discussions and suggestions. We also thank Jie Zhang for his help in providing and interpreting the LASCO data, and the anonymous referee for valuable comments in improving the manuscript. This work was supported by RHESSI PI funding.

REFERENCES

Antiochos, S. K. 1998, ApJ, 502, 181

Antiochos, S. K., Devore, C. R., Klimchuk, J. A. 1999, ApJ, 510, 485

Antonucci, E., Dodero, M. A., & Martin, R. 1990, ApJ, Sup., 73, 147

Bruzek, A. 1964, ApJ, 140, 746

Carmichael, H. 1964, In The Physics of Solar Flares, ed. W. N. Hess (NASA SP-50, Washington, DC:NASA), 451

Ciaravella, A., Raymond, J. C., Li, J., Reiser, P., Gardner, L. D., Ko, Y.-K., & Fineschi, S. 2002, ApJ, 575, 1116

Cheng, C. C. 1977, ApJ, 213, 558

Fletcher, L., & Hudson, H. S. 2002, Sol. Phys., 210, 307

Forbes, T. G., & Priest, E. R. 1984, Reconnection in solar flares. In: Butler, D.M., Papadopoulous, K. (Eds), Solar Terrestrial Physics: Present and Future, NASA, pp. 1-35.

Forbes, T. G., & Priest, E. R. 1995, ApJ, 446, 377

Forbes, T. G., & Acton, T. W. 1996, ApJ, 459, 330

Forbes, T. G., & Lin, J. 2000, J. of Atmos. and Sol.-Terr. Phys., 62, 1499

Gallagher, P. T., Dennis, B. R., Krucker, S., Schwartz, R. A., & Tolbert, A. K. 2002, Sol. Phys., 210, 341

Hirayama, T. 1974, Sol. Phys., 34, 323

Hirose, S., Uchida, T., Uemura, S., Yamaguchi T., & Cable, S.B. 2001, ApJ, 551, 586

Hood, A.W., & Priest, E.R. 1979, Sol. Phys., 64, 303

Hudson, H. S. 2000, ApJ, 531, L75

Hurford, G. J., et al. 2002, Sol. Phys., 210, 61

Hurford, G. J., Schwartz, R. A., Krucker, S., Lin, R. P., Smith, D. M., & Vilmer, N. 2003, ApJ, 595, L77

Ko, Y.-K., Raymond, J.C, Lin, J., Lawrence G., Li, J., Fludra, A. 2003, ApJ, 594, 1068

Kopp, R. A., & Pneuman, G. W. 1976, Sol. Phys., 50, 85

Krucker, S., Hurford, G. J., Lin, R.P. 2003, ApJ, 595, L103

Lin, R. P., et al. 2002, Sol. Phys., 210, 3

Lin, J., Forbes, T.G., Priest, E. R., & Bungey, T.N. 1995, Sol. Phys., 159, 275

Lin, J., & Forbes, T.G. 2000, J. Geophys. Res., 105, 2375

Lin, J. 2002, Chinese J. Astron. Astrophys., 2, 539

Lin, J. 2004, Sol. Phys., in press

Liu, W., Jiang, Y., Liu, S., & Petrosian, V. 2004, ApJ, submitted

Masuda, S., Kosugi, T., Hara, H., Tsuneta, S., & Ogawara, Y. 1994, Nature, 371, 495

Masuda, S., Kosugi, T., Hara, H., Sakao, T., Shibata, K., & Tsuneta, S. 1995, Publ. Astron. Soc. Japan, 47, 677

McKenzie, D.E. 2002, in Multi-Wavelength Observations of Coronal Structure and Dynamics, ed. Martens, P.C.H., Cauffman, D.P., 155

Moore, R., McKenzie, D.L., Švestka, Z., Widing, K.G., & 12 co-authors 1980, in P.A. Sturrock (ed), Solar Flares, A Monograph from Skylab Solar Workshop II, p. 341

Moore, R.L., & Roumeliotis, G. 1992, in Eruptive Solar Flares, (Z. Svestka, G.V. Jackson, M.E. Machaodo, eds.), Lecture Notes in Physics, 399, 69

Ohyama, M., & Shibata, K. 1998, ApJ, 499, 934

Parker, E. N. 1957, Sweet's mechanism for merging magnetic field in conducting fluids, J. Geophys. Res., 62, 509

Petschek, H. E. 1964, Magnetic field annihilation, in Physics of Solar Flares, ed. W. N. Hess (NASA SP-50, Washington, DC) pp. 425-439

Priest, E. R., & Forbes, T. G. 1990, Magnetic Reconnection: MHD Theory and Applications, Cambridge University Press, Cambridge, UK

Qiu, J., Wang, H., Cheng, C. Z., Gary, D. E., 2003, ApJ, 604, 900

Sakao, T., Kosugi, T., & Masuda, S. 1998, in ASSL Vol. 229, Observational Plasma Astrophysics: Five Years of Yohkoh and Beyond, ed. T. Watanabe, T. Kosugi, & A. C. Sterling (Boston: Kluwer), 273

Shibata, K., Masuda, S., Shimojo, M., Hara, H., Yokoyama, T., Tsuneta, S., Kosugi, T., & Ogawara, Y. 1995, ApJ, 451, 83

Shibata, K. 1999, Ap&SS, 264, 129

Smith, D. M., et al. 2002, Sol. Phys., 210, 33

Sturrock, P. A., 1966, Nature, 211, 695

Sui, L., & Holman, G. D. 2003, ApJ, 596, L251

Sui, L., & Holman, G. D., White, S. M., Gary, D. E., & Shibasaki, K., 2004, in prepration

Švestka, Z., Fontenla, J. M., Machado, M. E., Martin, S. T., Neidig, D. F. and Poletto, G. 1987, Sol. Phys., 169, 403

Švestka, Z. 1996, Sol. Phys., 108, 237

Tsuneta, S., Hara, H., Shimizu, T., Acton, L. W., Strong, K. T., Hudson, H. S., & Ogawara, Y. 1992, PASJ, 44, 63

Sweet, P. A. 1958, The production of high-energy particles in solar flares, Nuovo Cimento Suppl. 8, Ser. X, 188-196.

Tsuneta, S. 1996, ApJ, 456, 840

Tsuneta, S., Masuda, A., Kosugi, T., & Sato, J. 1997, ApJ, 478, 787

Uchida, Y., et al. 1999, Ap&SS, 264, 145

Veronig, A. M., Brown, J. C. 2004, ApJ, 603, L117

Veronig, A. M., Brown, J. C., Dennis, B. R., Schwartz, R. A., Sui, L., & Tolbert, A. K. 2004, ApJ, in prepration

Webb, D. F., Burkepile, J., Forbes, T. G., & Riley P. 2003, J. Geophys. Res., V108, Issue A12, pp. SSH 6-1

This preprint was prepared with the AAS LaTeX macros v5.2.

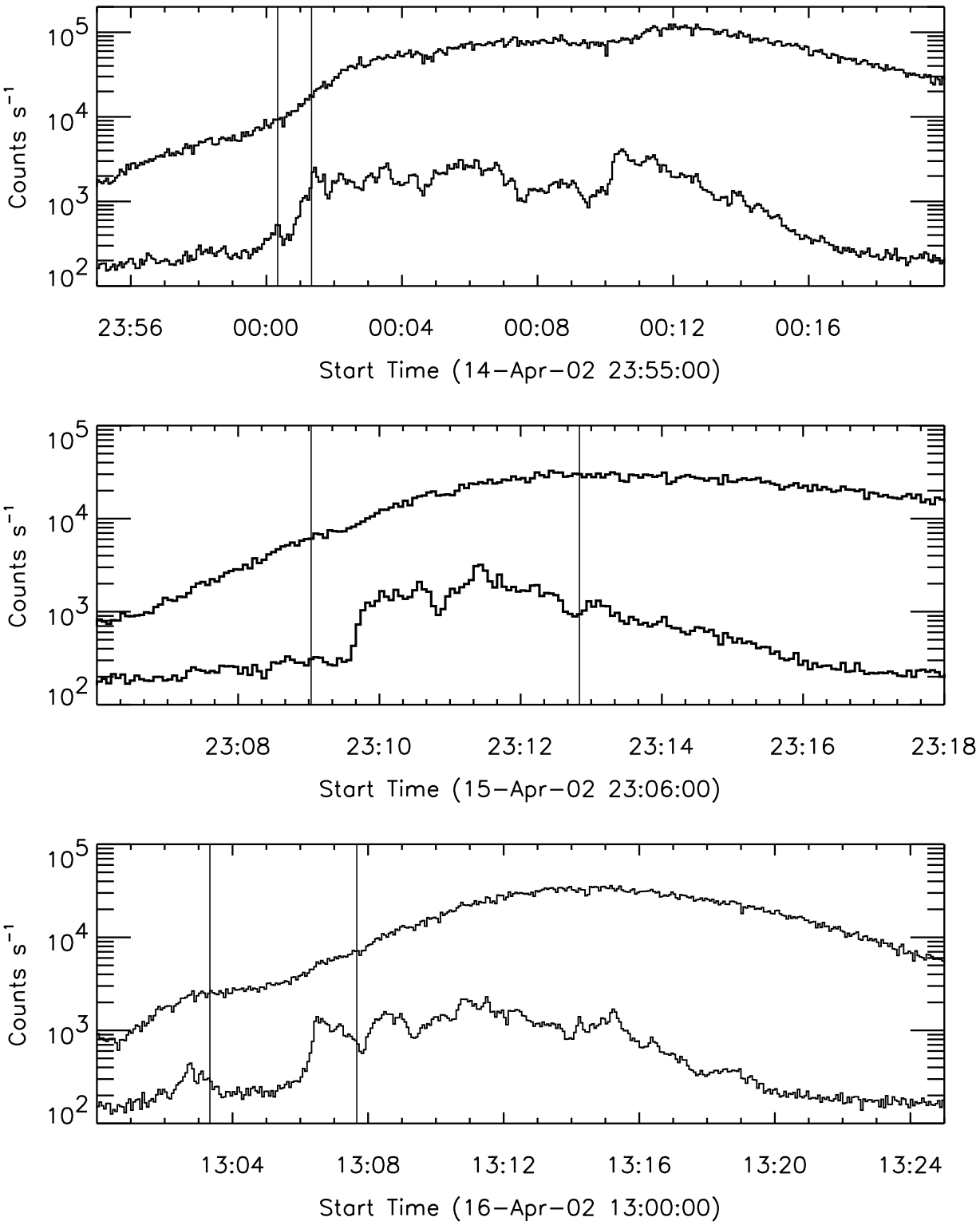

Fig. 1.— RHESSI light curves of the three flares. From *Top panel* to *Bottom panel* are the light curves of the April 14-15, 15, and 16 flares, respectively. The energy bands in each panel are 6-12 (upper curve) and 25-50 keV (lower curve). The solid lines in each panel mark the time range for the images in Fig. 2, 5, and 8. The time range was selected to show the RHESSI images with the coronal source above the flare loop.

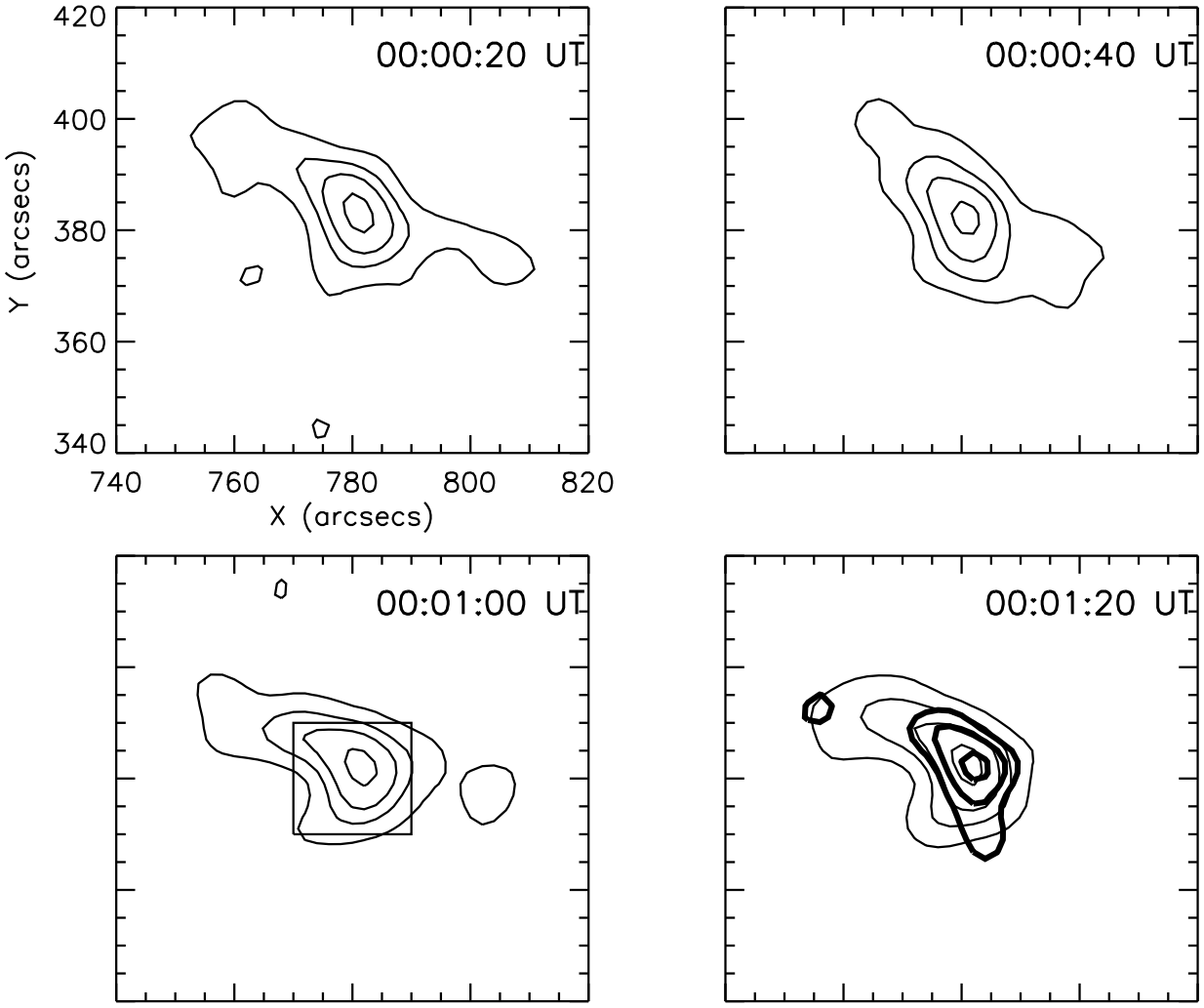

Fig. 2.— A sequence of 12-25 keV RHESSI images at the time of the impulsive rise of the 2002 April 14-15 flare (see Fig. 1 top panel). The time in each box is the start time of the 20s integration time interval (∼5 RHESSI rotation periods). RHESSI grids 3-9 were used, giving an angular resolution $\sim 7''$. The contour levels are 20%, 40%, 60%, and 90% of the peak flux in each image. The box in the image at 00:01:00 UT delineates the size of the image in Figure 4. The thick contours overplotted on the image at 01:20 UT are for the 25-50 keV band at 40%, 60%, and 90% the peak flux. Start times of images are indicated. The accumulation time of each images is 20 s.

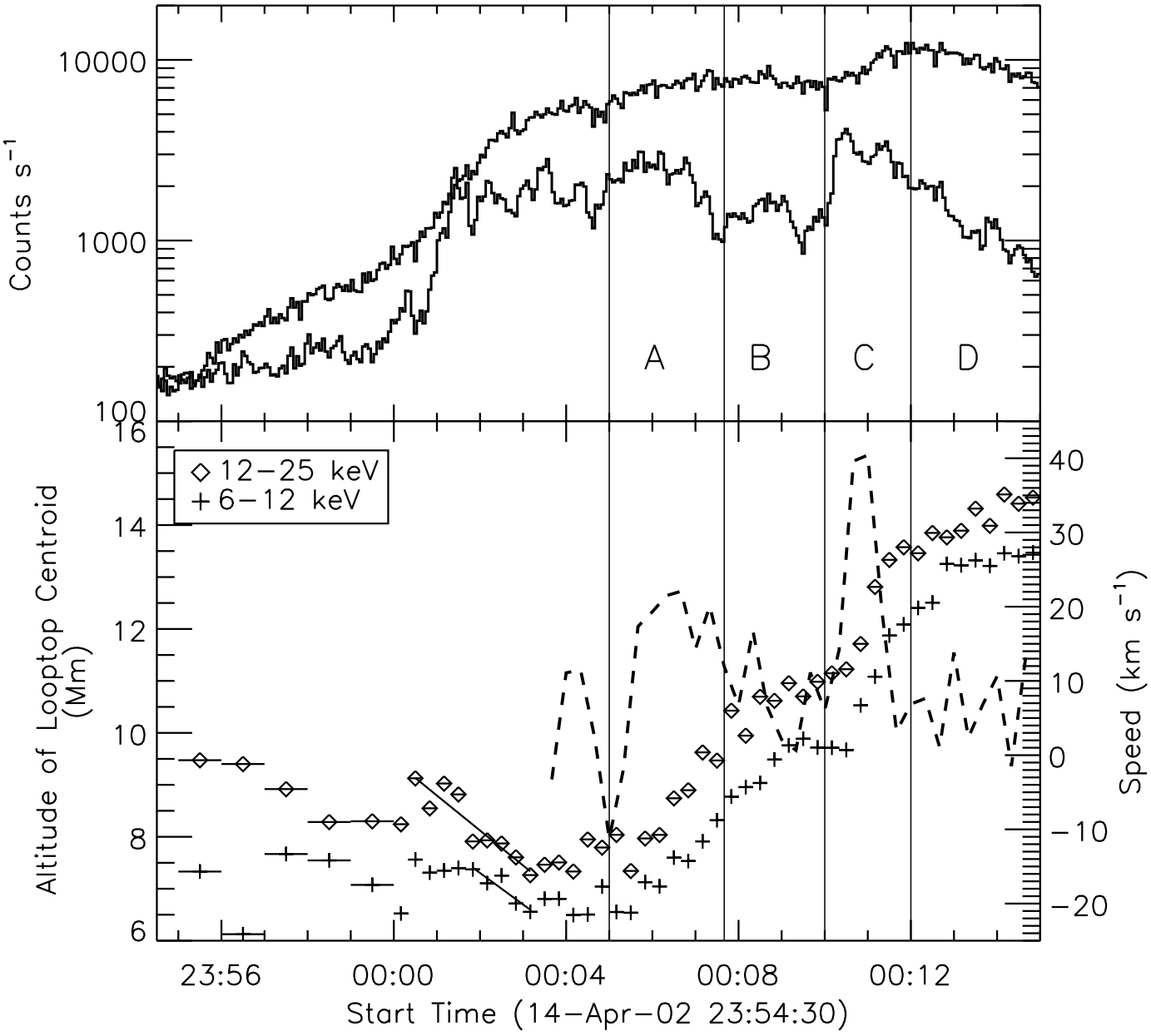

Fig. 3.— *Upper panel*: light curves in two energy bands (upper curve: 6-12 keV rate ×0.1, lower curve: 25-50 keV rate ×1.0) for the 2002 April 14-15 flare. *Lower panel*: altitude of the looptop centroid within the 60% contour for the images in the 6-12 keV band (plus) and 12-25 keV band (diamond). The horizontal bars on each point represents the integration time of the corresponding image. The solid lines show linear fits to the altitudes vs. time for two time ranges and two energy bands. The dashed line represents the apparent velocity of the looptop, determined by taking the time derivative of the 12-25 keV altitude curve after 00:03:50 UT.

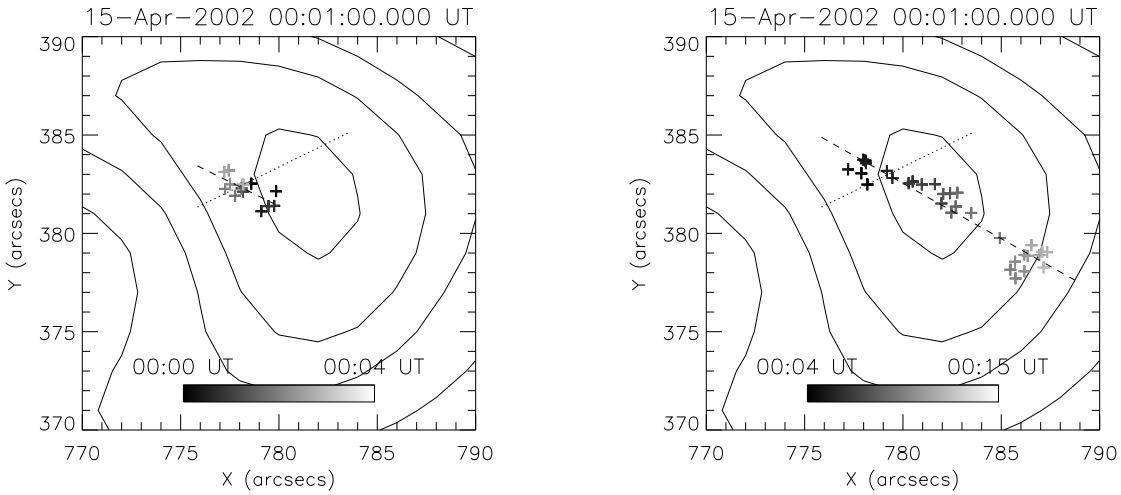

Fig. 4.— Looptop centroids (plus signs) overlaid on the looptop region contours of that 12-25 keV image of the April 14-15 flare at 00:01:00 UT shown in Figure 2. The *left panel* and the *right panel* show the centroids moving downward before 00:04 UT and upward after 00:04 UT, respectively. In both panels, the dotted lines represent the radial direction, while the dashed lines, which are from a linear fit to the centroid locations, represents the direction of motion. The angles between the radial direction and the direction of motion are 53° (*left panel*) and 56° (*right panel*). See online version for the figure in colors.

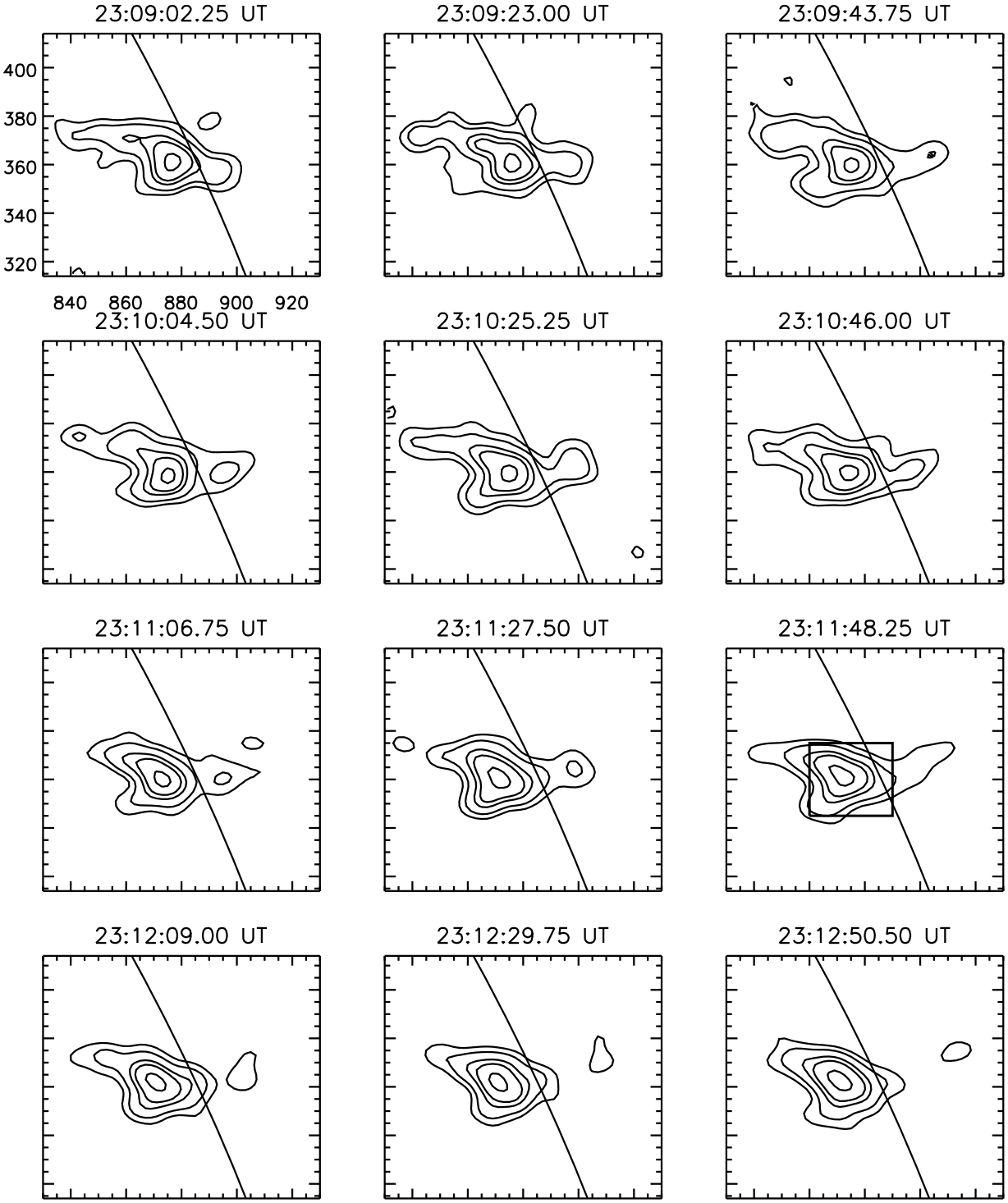

Fig. 5.— A time sequence of 10-25 keV RHESSI images for the 2002 April 15 flare. The imaging parameters are the same as those used in Figure 2. The contour levels are 15%, 25%, 45%, 60%, and 90% of the peak flux in each image. The box in the image at 23:11:48.25 UT delineates the size of the image view in Figure 7. The solid line denotes the solar limb.

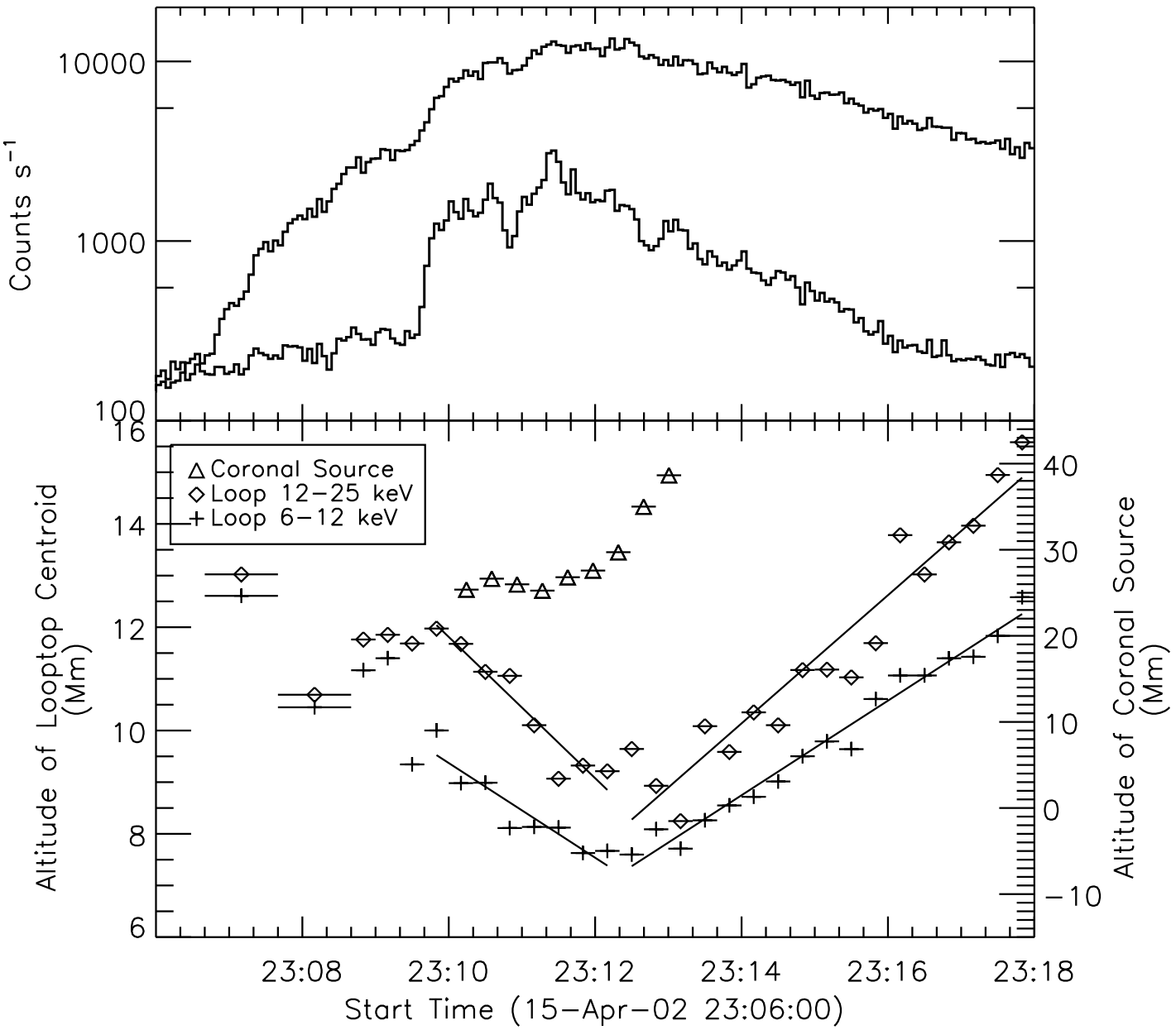

Fig. 6.— *Upper panel*: light curves in two energy bands (upper curve: 6-12 keV rate ×0.5, lower curve: 25-50 keV ×1.0) of the 2002 April 15 flare. *Lower panel*: altitude of the looptop centroid obtained using the 60% contour for the images in the 6-12 keV band (plus) and 12-25 keV band (diamond). The triangles show the altitude of the coronal source above the flare loop. The horizontal bars on each point represents the integration time of the corresponding image. The lines show linear fits to the altitudes vs. time for two time ranges and two energy bands.

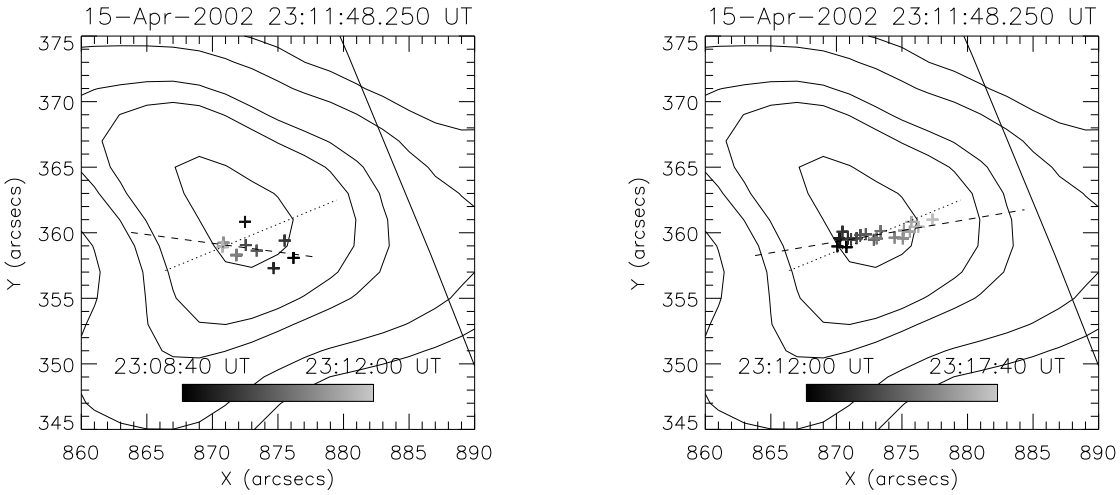

Fig. 7.— Looptop centroids (plus signs) overlaid on the looptop region of the 10-25 keV image of the April 15 flare at 23:11:48.25 UT shown in Figure 5. The other aspects of the figure are the same as for Fig. 4. The angles between the radial direction and the direction of motion are 30° (*left panel*) and 13° (*right panel*). See online version for the figure in colors.

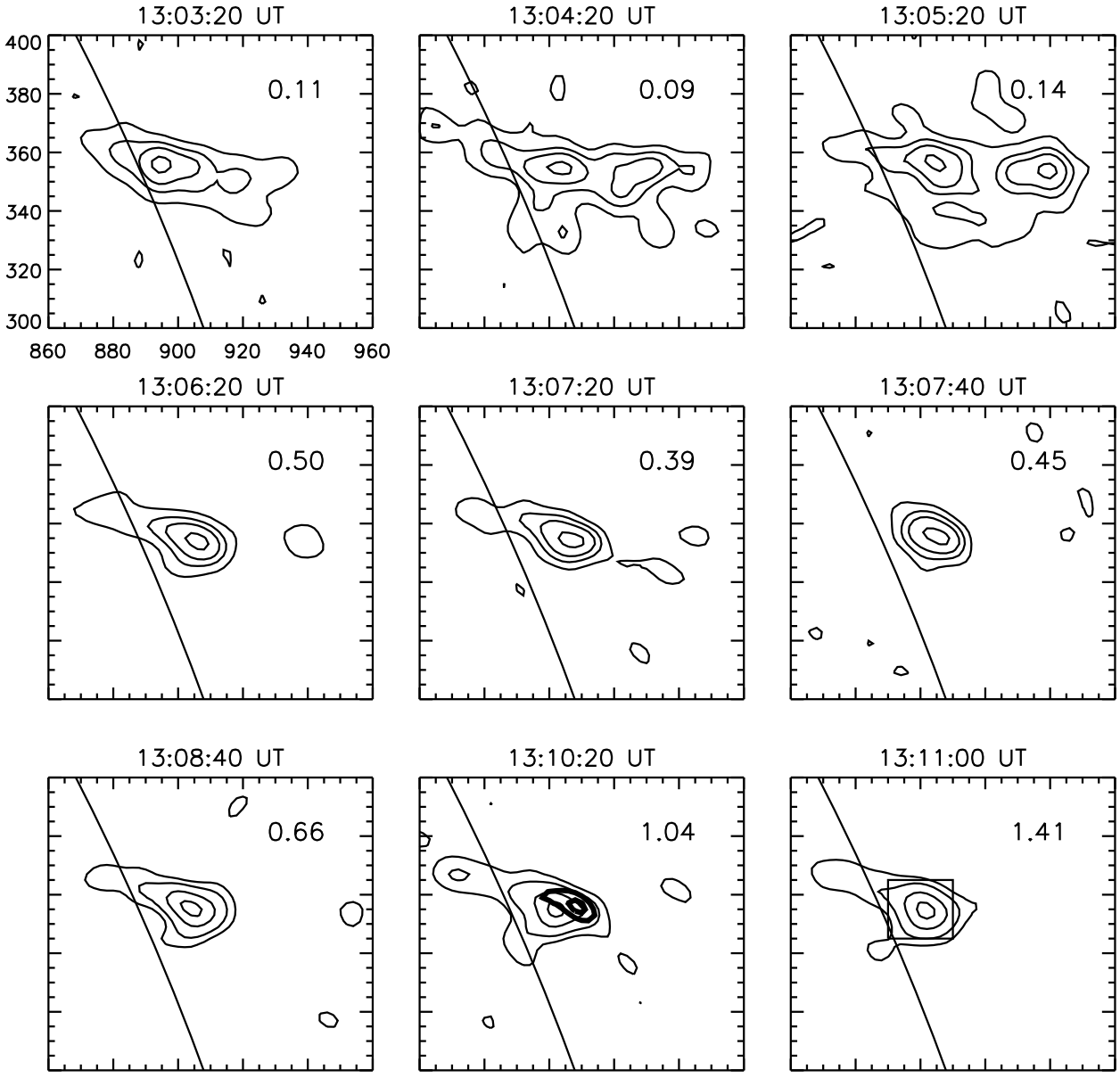

Fig. 8.— RHESSI 12-25 keV images for the April 16 flare. The imaging parameters are the same as those used in Figure 2. The integration time of the images was 1 min before and 20s after 13:07:20 UT. For the top two rows, the contour levels are 20%, 40%, 60%, and 90% of the peak flux in each image. For the bottom row, the contour levels are 15%, 30% , 60% and 90%. A RHESSI 25-50 keV image at 13:10:20 UT (contour levels showing 60%, and 90% of the peak flux) is plotted on the 12-25 keV image at the same time. The number on each image is the peak flux ($cm^{-2}s^{-1}arcsec^{-2}$) in 2 arcsec pixels. The box in the image at 13:11:00 UT delineates the size of the image view in Figure 10.

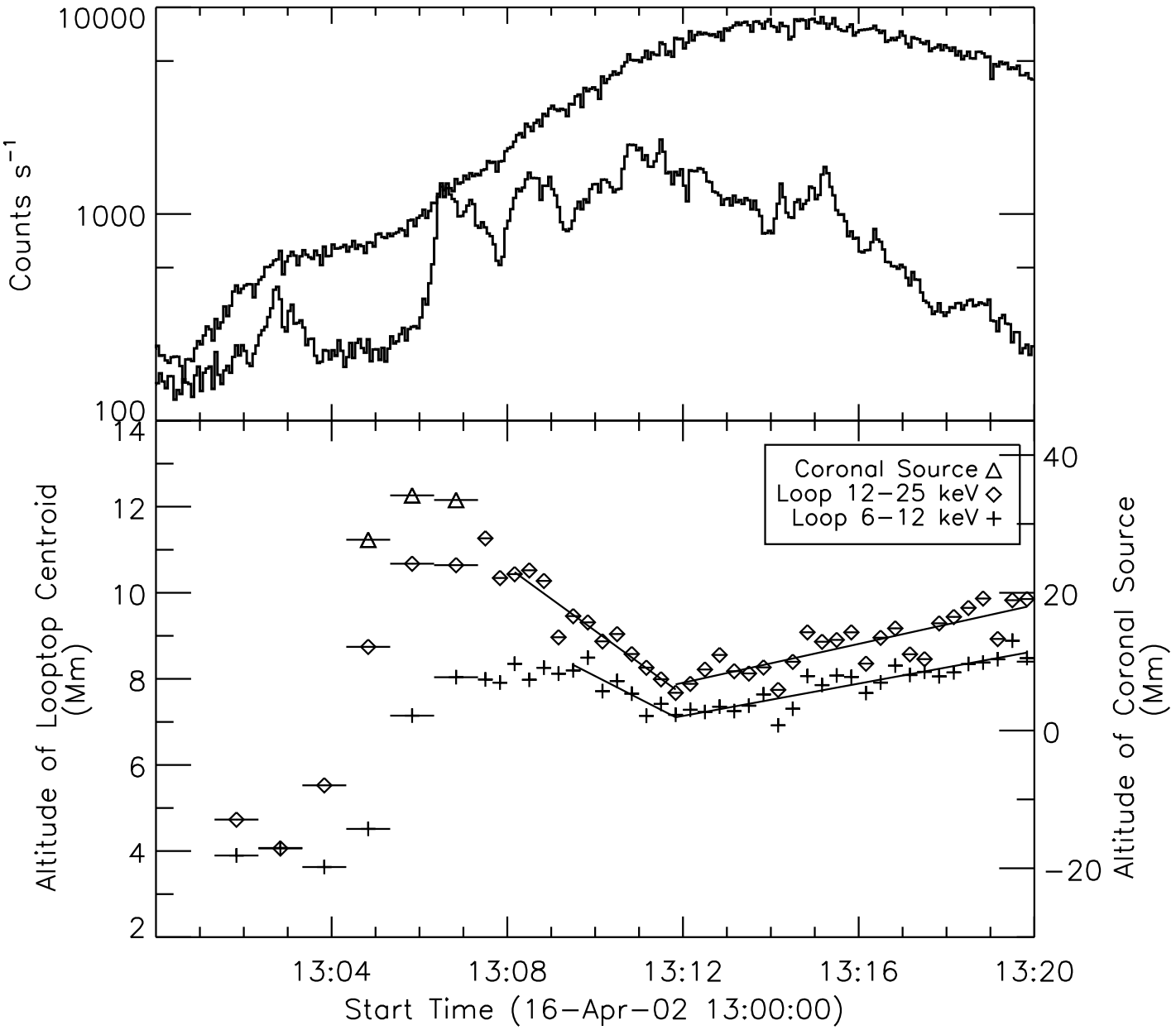

Fig. 9.— *Upper panel*: light curves in two energy bands (top curve: 6-12 keV, bottom curve: 25-50 keV) for the 2002 April 16 flare. The scale factors are 0.25 (6-12 keV) and 1.0 (12-25 keV). *Lower panel*: altitude of the looptop centroid obtained using the 60% contour of the flare looptop in the 6-12 keV band (plus signs) and 12-25 keV band (diamonds). The horizontal bars on each point represents the integration time of the corresponding image. The lines show linear fits to the altitudes vs. time for two time ranges and two energy bands. The triangles show the altitude of the coronal source above the flare loop.

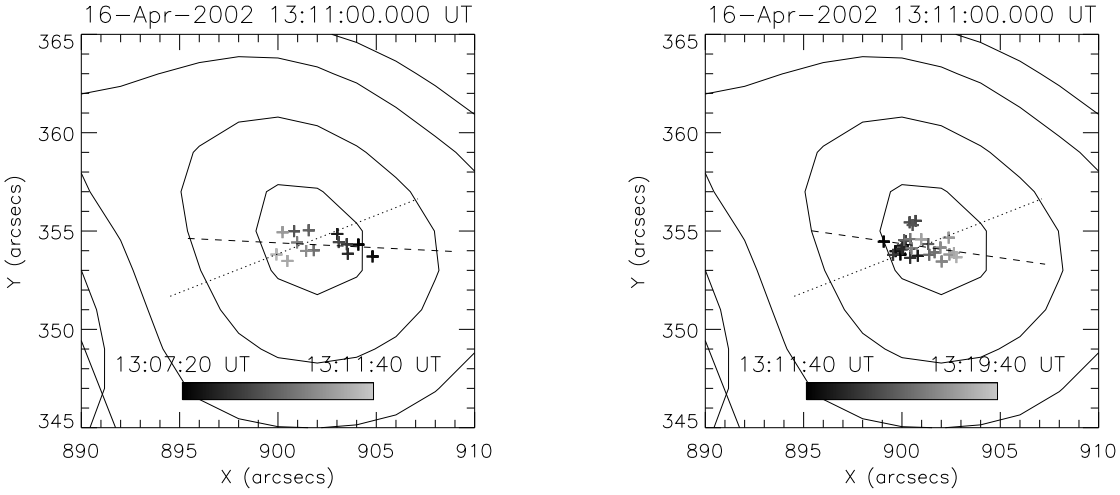

Fig. 10.— Looptop centroids (plus signs) overlaid on the looptop region of the 12-25 keV image of the April 16 flare at 13:11:00 UT in Figure 8. The other aspects of the figure are the same as in Fig. 4. The angles between the radial direction and the direction of motion are 24° (*left panel*) and 30° (*right panel*). See online version for the figure in colors.

Table 1. Summary of the three flares.

Date	April 14-15	April 15	April 16
GOES Class	M3.7	M1.2	M2.5
Location (deg)	N20 W53	N22 W69	N21 W71
Start Time (UT)	23:50:00	23:00:00	12:50:00
SXR Peak (UT)	00:08:00	23:14:00	13:18:00
End Time (UT)	00:50:00	23:20:00	13:40:00
Peak Temperature* (MK)	24	32	24
Peak Emission Measure ($10^{48} cm^{-3}$)	6	0.4	3.5
CME Association	No	Yes	No
CME Speed(km/s)	...	300	...

*The peak plasma temperature and emission measure were obtained by fitting RHESSI spatially integrated spectra.

Table 2. Summary of the RHESSI observations of the three flares.

Date	Looptop* (Downward)			Looptop**(Upward)	Coronal Source	
	Initial Altitude (Mm)	Decrease (%)	Speed (km/s)	Speed (km/s)	Initial Altitude (Mm)	Speed (km/s)
April 14-15	7.5 / 9	13 / 20	10 / 11	3∼35 / 5∼40	27	···
April 15	10 / 12	24 / 23	15 / 23	15 / 21	25	300
April 16	8.5 / 11	16 / 30	8 / 12	3 / 4	31	···

*The first and second numbers are for 6-12 and 12-25 keV, respectively.

**The speed range of the upward motion for the April 14-15 flare was obtained by taking the time derivative of the altitudes in both the 6-12 and 12-25 keV bands.